Bit-Interleaved Coded Multiple Beamforming with Perfect Coding in Millimeter-Wave MIMO Systems

Sadjad Sedighi, *Student Member, IEEE,* and Ender Ayanoglu, *Fellow, IEEE*

CPCC, Dept of EECS, UC Irvine, Irvine, CA, USA,

***Abstract*— This letter investigates bit-interleaved coded multiple beamforming (BICMB) with perfect coding in millimeter-wave (mm-wave) multiple-input multiple-output (MIMO) systems to achieve the maximum diversity gain. Using perfect coding with BICMB enables us to do this. We show that by using BICMB and perfect coding, the diversity gain becomes independent of the number of transmitted data streams and the number of antennas in each remote antenna unit (RAU) at the transmitter and the receiver. The assumption is that the perfect channel state information (CSI) is known at both the transmitter and the receiver. With the assumption of the perfect CSI at the transmitter and the receiver, simulation results show that the use of BICMB with perfect coding results in the diversity gain values predicted by the analysis.**

I. Introduction

Diversity gain analysis of a millimeter-wave (mm-wave) multiple-input multiple-output (MIMO) system with distributed antenna-subarray (DAS) architecture was first studied in [1]. The diversity gain calculated in [1] depends on the number of transmitted data streams in the system. This means by increasing the number of transmitted data streams, the diversity gain decreases. Furthermore, the diversity gain in [1] can be increased simply by increasing the number of antenna subarrays. Diversity gain analysis for the mm-wave MIMO systems is studied in [2].

Bit-interleaved coded modulation (BICM) was first introduced to increase the code diversity [3], [4]. Later on, bit-interleaved coded multiple beamforming (BICMB) was used to achieve full diversity gain and full multiplexing gain in MIMO systems [5], [6]. In this method, different codewords are interleaved among different subchannels with different diversity orders. To overcome this diversity degradation, in [7], we proved that by using BICMB in a mm-wave massive MIMO system with DAS architecture both full diversity gain and full multiplexing gain can be achieved.

Perfect space-time block codes (PSTBC) were studied in [8], [9] to achieve full rate and full diversity in any dimension. However, dimensions 2, 3, 4 and 6 are the only dimensions that can achieve an increase in the coding gain. In [10], perfect coding with multiple beamforming is used to achieve full diversity and full multiplexing in a MIMO system with less decoding complexity than a system employing PSTBC and full precoded multiple beamforming (FPMB). In [11], channel coding is added to the perfect coding and diversity gain analysis is carried out to prove that BICMB with perfect coding (BICMB-PC) achieves the full diversity order.

Space-time block codes (STBC) are studied in massive MIMO literature. In [12], space-time block codes are used to achieve full diversity gain in a flat fading non-coherent wireless communication system. Also, in [13] massive space-time block code (MaSTBC) is studied. Authors in [13] proposed a novel space-time modulation scheme with PSK modulated MaSTBC for multi-user massive MIMO uplink systems.

In this work, we use BICMB-PC to achieve full diversity gain in mm-wave MIMO systems. The diversity analysis for this system is carried out. We show that by using perfect coding in addition to convolutional coding, the diversity gain becomes independent of the number of transmitted data streams.

II. System Model

One can approximate the average probability of bit error rate (BER) P_E at high SNR regimes for both coded and uncoded systems as [14], [15]

$$P_E \approx (G_c \bar{\gamma})^{-G_d}, \tag{1}$$

where G_c and G_d are defined as coding gain and diversity gain, respectively. Note that diversity gain is not a property of high SNR regimes. Average SNR is shown by $\bar{\gamma}$. In a log-log scale, diversity gain G_d determines the slope of the BER versus the average SNR curve in high SNR regime. Furthermore, changing G_c leads to shift of the curve in SNR relative to a benchmark BER curve of $(\bar{\gamma}^{-G_d})$. In this work, our focus is on calculating the diversity gain and we leave the coding gain for future work.

We consider a single-user mm-wave MIMO scenario shown in Fig. 1, where the transmitter is equipped with M_t RAUs, N_t antennas at each RAU, and N_t^{RF} RF chains. The receiver has M_r RAUs, N_r antennas at each RAU, and N_r^{RF} RF chains. The transmitter sends $N_s = D$ data streams to the receiver. These data streams are generated as follows. First the bit codeword $\mathbf{c}$ is generated through a convolutional encoder with code rate R_c. Then a random bit-interleaver is used to generate an interleaved sequence. The output of the interleaver is modulated by M-quadrature amplitude modulation (M-QAM). We define a one-to-one mapping from $\mathbf{X}_k = \left[\mathbf{x}_{1,k}, \ldots, \mathbf{x}_{D,k}\right]$ to $\mathbf{Z}_k$ as $\mathbf{Z}_k = \mathbb{M}\{\mathbf{X}_k\}$ where $\mathbb{M}$ denotes the PSTBC codeword

This work was partially supported by NSF under Grant No. 1547155.

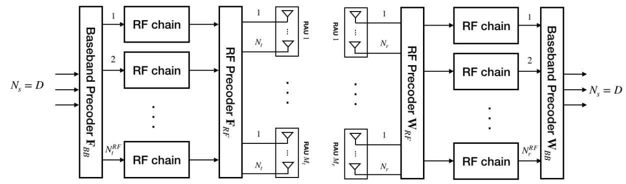

Fig. 1. Block diagram of a mm-wave MIMO system with distributed antenna sub-arrays.

generating function [11]. A PSTBC codeword, i.e., $\mathbf{Z}_k$ is generated by using D^2 consecutive complex-valued scalar symbols [11]

$$\mathbf{Z}_k = \mathbb{M}\{\mathbf{X}_k\} = \sum_{v=1}^{D} \mathrm{diag}(\mathbf{G}\mathbf{x}_{v,k})\mathbf{E}^{v-1}, \tag{2}$$

where $\mathbf{G}$ is an $D \times D$ unitary matrix [8], $\mathbf{x}_{v,k}$ is a $D \times 1$ vector whose elements are the vth D input modulated scalar symbols and $D \in \{2,3,4,6\}$. Matrix $\mathbf{E}$ is defined as

$$\mathbf{E} = \begin{bmatrix} 0 & 1 & 0 & \cdots & 0 & 0 \\ 0 & 0 & 1 & \cdots & 0 & 0 \\ \vdots & \vdots & \vdots & \ddots & \vdots & \vdots \\ 0 & 0 & 0 & \cdots & 0 & 1 \\ g & 0 & 0 & \cdots & 0 & 0 \end{bmatrix}, \tag{3}$$

where

$$g = \begin{cases} i, & D = 2,4, \\ e^{\frac{2\pi}{3}}, & D = 3, \\ -e^{\frac{2\pi}{3}}, & D = 6. \end{cases} \tag{4}$$

As it can be seen from Fig. 1, the complex-valued matrix $\mathbf{F}_{\mathrm{BB}} \in \mathbb{C}^{N_t^{RF} \times N_s}$ is used for preprocessing at the baseband. A set of $M_t N_t$ phase shifters is applied to the output of each RF chain. As a result of this process, different beams are formed in order to transmit the RF signals. We can model this process with a complex-valued matrix $\mathbf{F}_{\mathrm{RF}} \in \mathbb{C}^{M_t N_t \times N_t^{RF}}$. Note that in this work $M_t = M_r = N_s = D$.

By assuming a narrowband flat fading channel model, we write the $M_r N_r \times M_t N_t$ channel matrix $\mathbf{H}$ as

$$\mathbf{H} = \begin{bmatrix} \sqrt{\beta_{11}}\mathbf{H}_{11} & \ldots & \sqrt{\beta_{1M_t}}\mathbf{H}_{1M_t} \\ \vdots & \ddots & \vdots \\ \sqrt{\beta_{M_r 1}}\mathbf{H}_{M_r 1} & \ldots & \sqrt{\beta_{M_r M_t}}\mathbf{H}_{M_r M_t} \end{bmatrix}, \tag{5}$$

where each $\mathbf{H}_{ij}$ is the MIMO channel between the ith RAU at the receiver and the jth RAU at the transmitter. Also, β_{ij} is a real-valued nonnegative number and represents the large-scale fading effect between the ith RAU at the receiver and jth RAU at the transmitter. Note that in this work, we use Saleh-Valenzuela model for each subchannel $\mathbf{H}_{ij}$ [7], [16]. For the sake of simplicity, each scattering cluster is assumed to contribute a single propagation path. The subchannel matrix $\mathbf{H}_{ij}$ is given by

$$\mathbf{H}_{ij} = \sqrt{\frac{N_t N_r}{L_{ij}}} \sum_{l=1}^{L_{ij}} \alpha_{ij}^{l} \mathbf{a}_r(\theta_{ij}^{l}) \mathbf{a}_t^{H}(\phi_{ij}^{l}), \tag{6}$$

where L_{ij} is the number of propagation paths and α_{ij}^{l} is the complex-gain of the lth ray which follows $\mathcal{CN}(0,1)$, $\theta_{ij}^{l} \in [0, 2\pi]$, $\phi_{ij}^{l} \in [0, 2\pi]$, for all i, j, l, and the vectors $\mathbf{a}_r(\theta_{ij}^{l})$ and $\mathbf{a}_t(\phi_{ij}^{l})$ are the normalized array response at the receiver and transmitter, respectively. In particular, this paper adopts a uniform linear array (ULA) where both $\mathbf{a}_r(\theta_{ij}^{l})$ and $\mathbf{a}_t(\phi_{ij}^{l})$ are modeled as

$$\mathbf{a}_{\mathrm{ULA}}(\varphi) = \frac{1}{\sqrt{N}} \left[1, e^{j\frac{2\pi}{\lambda} d \sin(\varphi)}, \ldots, e^{j(N-1)\frac{2\pi}{\lambda} d \sin(\varphi)}\right]^{T}, \tag{7}$$

where λ is the transmission wavelength, and d is the antenna spacing.

The processed signal at the kth PSTBC codeword is

$$\mathbf{Y}_k = \mathbf{W}_{\mathrm{BB}}^{H} \mathbf{W}_{\mathrm{RF}}^{H} \mathbf{H} \mathbf{F}_{\mathrm{RF}} \mathbf{F}_{\mathrm{BB}} \mathbf{Z}_k + \mathbf{W}_{\mathrm{BB}}^{H} \mathbf{W}_{\mathrm{RF}}^{H} \mathbf{n}_k, \tag{8}$$

where $\mathbf{Y}_k$ is an $D \times D$ complex-valued matrix, $\mathbf{n}_k$ is an $M_r N_r \times 1$ vector consisting of i.i.d. $\mathcal{CN}(0, N_0)$ noise samples, $N_0 = \frac{N_t}{SNR}$ where SNR is defined as the signal-to-noise ratio (SNR), $\mathbf{W}_{\mathrm{RF}}$ is the $M_r N_r \times N_r^{RF}$ RF combining matrix, and $\mathbf{W}_{\mathrm{BB}}$ is the $N_r^{(\mathrm{RF})} \times N_s$ baseband combining matrix.

A solution based on singular value decomposition (SVD) of the channel matrix $\mathbf{H} = \mathbf{U}\mathbf{\Lambda}\mathbf{V}^{H}$ can be derived for the beamforming matrices [7]. By utilizing the optimal precoder and combiner, one can write (8) as

$$\mathbf{Y}_k = \mathbf{\Lambda}\mathbf{Z}_k + \tilde{\mathbf{n}}_k, \tag{9}$$

where $\tilde{\mathbf{n}}_k = \mathbf{U}_{(1:D)}^{H} \mathbf{n}_k$, and $\mathbf{U}_{(1:D)}$ is the first D columns of the unitary matrix $\mathbf{U}$.

We model the PSTBC codeword sequence as $k' \to (k, (m,n), j)$, where k' represents the original ordering of the coded bits $c_{k'}$, $(k, (m,n), j)$ are the index of the PSTBC codewords, the symbol position in $\mathbf{X}_k$, and the bit position on the label of the scalar symbol $x_{(m,n),k}$, respectively. We define χ_b^j as the subset of all signals $x \in \chi$. Note that the label has the value $b \in \{0,1\}$ in position j.

The maximum likelihood (ML) bit metrics for (8) can be written as

$$\gamma^{(m,n),j}(\mathbf{Y}_k, c_{k'}) = \min_{\mathbf{X} \in \eta_{c_{k'}}^{(m,n),j}} ||\mathbf{Y}_k - \Lambda\mathbb{M}\{\mathbf{X}\}||^2, \tag{10}$$

where $\eta_{c_{k'}}^{(m,n),j}$ is defined as

$$\eta_{c_{k'}}^{(m,n),j} = \{\mathbf{X} : x_{(u,v)=(m,n)} \in \chi_b^j, \text{ and } x_{(u,v)\neq(m,n)} \in \chi\}. \tag{11}$$

The ML decoder at the receiver makes decisions according to the rule

$$\hat{\mathbf{c}} = \underset{\mathbf{c}}{\mathrm{argmin}} \sum_{k'} \gamma^{(m,n),j}(\mathbf{Y}_k, c_{k'}). \tag{12}$$

III. Diversity Gain Analysis

In this section, the diversity gain is examined for mm-wave MIMO systems employing DAS architecture employing BICMB-PC. We show that the diversity gain becomes independent of the number of transmitted streams, whereas in [1] the diversity gain is dependent on the number of transmitted data streams. This will be done by computing an upper bound for the pairwise error probability (PEP).

Theorem 1. Suppose that N_r and N_t are sufficiently large [7]. Then by utilizing BICMB-PC, mm-wave MIMO systems with DAS architecture can achieve a diversity gain of

$$G_d = \frac{\left(\sum_{i,j} \beta_{ij}\right)^2}{\sum_{i,j} \beta_{ij}^2 L_{ij}^{-1}} \tag{13}$$

for $i = 1, \ldots, M_r$ and $j = 1, \ldots, M_t$.

Proof. Assume that codeword $\mathbf{c}$ is transmitted and codeword $\hat{\mathbf{c}}$ is detected. Then one can write the PEP of $\mathbf{c}$ and $\hat{\mathbf{c}}$ as

$$P(\mathbf{c} \to \hat{\mathbf{c}}|\mathbf{H}) = P\left(\sum_{k'} ||\mathbf{Y}_k - \Lambda\tilde{\mathbf{Z}}\}||^2 \geq \sum_{k'} ||\mathbf{Y}_k - \Lambda\hat{\mathbf{Z}}\}||^2 \mid \mathbf{H}\right), \tag{14}$$

where $\tilde{\mathbf{Z}} = \mathbb{M}\{\tilde{\mathbf{X}}\}$, $\hat{\mathbf{Z}} = \mathbb{M}\{\hat{\mathbf{X}}\}$, $\tilde{\mathbf{X}} = \operatorname{argmin}_{\mathbf{X}\in\eta^{(m,n),j}_{c_{k'}}} ||\mathbf{Y}_k - \Lambda\mathbb{M}\{\mathbf{X}\}||^2$, and $\hat{\mathbf{X}} = \operatorname{argmin}_{\mathbf{X}\in\eta^{(m,n),j}_{\bar{c}_{k'}}} ||\mathbf{Y}_k - \Lambda\mathbb{M}\{\mathbf{X}\}||^2$. Since the bit metrics corresponding to the same coded bits between the pairwise errors are the same and $||\mathbf{Y}_k - \mathbf{\Lambda}\mathbf{Z}_k||^2 \geq ||\mathbf{Y}_k - \mathbf{\Lambda}\hat{\mathbf{Z}}_k||$, (14) is upper-bounded by

$$P(\mathbf{c} \to \hat{\mathbf{c}}|\mathbf{H}) \leq P\left(\xi \geq \sum_{k',d_H} ||\mathbf{\Upsilon}||^2\right) \tag{15}$$

where $\sum_{k',d_H}$ is the summation of the d_H values corresponding to the different coded bits between the bit codewords, $\mathbf{\Upsilon} = \mathbf{\Lambda}(\mathbf{Z} - \hat{\mathbf{Z}}_k)$, and $\xi = -\sum_{k',d_H} \operatorname{tr}\left(\mathbf{\Upsilon}^H \mathbf{n}_k + \mathbf{n}_k^H \mathbf{\Upsilon}\right)$. Since $\xi \sim \mathcal{CN}\left(0, 2N_0 \sum_{k',d_H} ||\mathbf{\Upsilon}||^2\right)$, (15) is replaced by the Q function as

$$P(\mathbf{c} \to \hat{\mathbf{c}}|\mathbf{H}) \leq Q\left(\sqrt{\frac{\sum_{k',d_H} ||\mathbf{\Upsilon}||^2}{2N_0}}\right). \tag{16}$$

By using an upper bound of the Q function $Q(x) \leq \frac{1}{2}e^{-\frac{x^2}{2}}$, the average PEP in is upper bounded as

$$P(\mathbf{c} \to \hat{\mathbf{c}}) = E[P(\mathbf{c} \to \hat{\mathbf{c}}|\mathbf{H})] \leq \frac{1}{2}E\left[\exp\left(-\frac{\sum_{k',d_H} ||\mathbf{\Upsilon}||^2}{4N_0}\right)\right]. \tag{17}$$

By using [10], we can rewrite (17) as

$$P(\mathbf{c} \to \hat{\mathbf{c}}) = \frac{1}{2}E\left[\exp\left(-\frac{\sum_{u=1}^{D} \lambda_u^2 \zeta_u}{4N_0}\right)\right], \tag{18}$$

where $\zeta_u = \sum_{k',d_H} \rho_{u,k}$ and $\rho_{u,k} = \sum_{v=1}^{D} |\mathbf{g}_u^T(\mathbf{x}_{v,k} - \hat{\mathbf{x}}_{v,k})|^2$.

By defining $L_t = \sum_{i,j} L_{ij}$ as the rank of the channel matrix $\mathbf{H}$, i.e., the number of singular values of the channel matrix $\mathbf{H}$, we can write

$$\frac{\left(\zeta_{\min} \sum_{u=1}^{L_t} \lambda_u^2\right)}{L_t} \leq \frac{\left(\zeta_{\min} \sum_{u=1}^{D} \lambda_u^2\right)}{D} \leq \frac{\left(\sum_{u=1}^{D} \lambda_u^2 \zeta_u\right)}{D}. \tag{19}$$

One can define

$$\Theta \triangleq \sum_{u=1}^{L_t} \lambda_u^2 = ||\mathbf{H}||_F^2 = \sum_{i=1}^{M_r}\sum_{j=1}^{M_t} \beta_{ij} ||\mathbf{H}_{ij}||_F^2. \tag{20}$$

When N_t and N_r are sufficiently large, the singular values of $\mathbf{H}_{ij}$ converge to $\sqrt{\frac{N_r N_t}{L_{ij}}}\left|\alpha_l^{ij}\right|$ in descending order [7]. Therefore, one can rewrite (20) as

$$\Theta = \sum_{i=1}^{M_r}\sum_{j=1}^{M_t} \beta_{ij} ||\mathbf{H}_{ij}||_F^2 = N_r N_t \sum_{i=1}^{M_r}\sum_{j=1}^{M_t} \underbrace{\frac{\beta_{ij}}{L_{ij}} \sum_{l=1}^{L_{ij}} \left|\alpha_{ij}^l\right|^2}_{\Psi_{ij}}. \tag{21}$$

Note that the random variable $\sum_{l=1}^{L_{ij}} \left|\alpha_{ij}^l\right|$ has a χ-squared distribution with $2L_{ij}$ degrees of freedom, or equivalently a Gamma distribution with shape L_{ij} and scale 2, i.e., $\mathcal{G}(L_{ij}, 2)$. Then, since $\beta_{ij} L_{ij}^{-1} > 0$, $\Psi_{ij} \sim \mathcal{G}(L_{ij}, 2\beta_{ij} L_{ij}^{-1})$ [17]. The Welch-Satterthwaite equation is used here to approximate the shape and scale of the Gamma distribution. One can see that Θ is a linear combination of the independent random variables Ψ_{ij} [18, p.4.1-1]. The shape and scale of Θ can be calculated as

$$\kappa = \frac{\left(\sum_{i,j} \theta_{ij} k_{ij}\right)^2}{\sum_{i,j} \theta_{ij}^2 k_{ij}} = \frac{\left(\sum_{i,j} \beta_{ij}\right)^2}{\sum_{i,j} \beta_{ij}^2 L_{ij}^{-1}}, \tag{22}$$

$$\theta = \frac{\sum_{i,j} \theta_{ij}^2 k_{ij}}{\sum_{i,j} \theta_{ij} k_{ij}} = \frac{\sum_{i,j} \beta_{ij}^2 L_{ij}^{-1}}{\sum_{i,j} \beta_{ij}}. \tag{23}$$

By using (19) and the definition of the moment generating function (MGF) [19], we can upper-bound the PEP in (17) by

$$P(\mathbf{c} \to \hat{\mathbf{c}}) \leq \frac{1}{2}E\left[\exp\left(\frac{-\zeta_{\min} D}{4N_0 L_t}\Theta\right)\right]. \tag{24}$$

By using MGF of Θ, (24) can be written as

$$P(\mathbf{c} \to \hat{\mathbf{c}}) \leq \frac{1}{2}\left(1 + \theta\frac{\zeta_{\min} D N_t}{4L_t} SNR\right)^{-\kappa} \tag{25}$$

$$\approx \frac{1}{2}\left(\theta\frac{\zeta_{\min} D N_t}{4L_t} SNR\right)^{-\kappa} \tag{26}$$

for high SNR.

Hence, BICMB-PC achieves full diversity order of

$$G_d = \kappa = \frac{\left(\sum_{i,j} \beta_{ij}\right)^2}{\sum_{i,j} \beta_{ij}^2 L_{ij}^{-1}} \tag{27}$$

which is independent of the number of transmitted data streams.

Remark 1. By assuming that $L_{ij} = L$ and $\beta_{ij} = \beta$ for any $i \in \{1, \ldots, M_r\}$ and $j \in \{1, \ldots, M_t\}$, it can be seen easily that the mm-wave MIMO system with DAS architecture can achieve a diversity gain

$$G_d = M_r M_t L = D^2 L. \tag{28}$$

One can compare this result with the diversity gain calculated for the single-user scenario in [1]. As it can be seen, similar to [7], the full diversity gain is achieved in this paper.

IV. Decoding

By replacing (2) in (9), we can rewrite (9) and show that each element of $\mathbf{\Lambda Z}_k$ is related to only one of the $\mathbf{x}_{v,k}$ [10], [11]. For the case $D = 3$, we can write

$$\mathbf{Y}_k = \begin{bmatrix} \lambda_1 \mathbf{g_1}^T \mathbf{x}_{1,k} & \lambda_1 \mathbf{g_1}^T \mathbf{x}_{2,k} & \lambda_1 \mathbf{g_1}^T \mathbf{x}_{3,k} \\ g\lambda_2 \mathbf{g_2}^T \mathbf{x}_{3,k} & \lambda_2 \mathbf{g_2}^T \mathbf{x}_{1,k} & \lambda_2 \mathbf{g_2}^T \mathbf{x}_{2,k} \\ g\lambda_3 \mathbf{g_3}^T \mathbf{x}_{3,k} & g\lambda_3 \mathbf{g_3}^T \mathbf{x}_{1,k} & \lambda_3 \mathbf{g_3}^T \mathbf{x}_{1,k} \end{bmatrix} + \tilde{\mathbf{n}}_k. \quad (29)$$

The processed signal in (29) can be divided into D parts. Then one can write

$$\mathbf{y}_{v,k} = \mathbf{\Omega}_v \mathbf{\Lambda G x}_{v,k} + \tilde{\mathbf{n}}_{k,v} \quad (30)$$

where $v = 1, \dots, D$ and $\mathbf{\Omega}_v = \mathrm{diag}(\omega_{v,1}, \dots, \omega_{v,D})$. The elements of the matrix $\mathbf{\Omega}_v$ are defined as

$$\omega_{v,u} = \begin{cases} 1, & 1 \le u \le D - v + 1 \\ g, & D - v + 2 \le u \le D. \end{cases} \quad (31)$$

One can simplify (30) by using the QR decomposition of $\mathbf{\Lambda G} = \mathbf{QR}$ as done in [11] to simplify the ML bit metrics defined in (10) as follows:

$$\gamma^{(m,n),j}(\mathbf{Y}_k, c_{k'}) = \min_{\mathbf{x} \in \rho^{n,j}_{c_{k'}}} ||\tilde{\mathbf{y}}_{m,k} - \mathbf{Rx}||^2, \quad (32)$$

where $\tilde{\mathbf{y}}_{m,k} = \mathbf{Q}^H \mathbf{\Omega}^H_m \mathbf{y}_{m,k}$, and $\rho^{n,j}_{c_{k'}}$ is a subset of χ^D. This subset is defined as

$$\rho^{n,j}_b = \{\mathbf{x} = [x_1, \dots, x_D]^T : x_{d=n} \in \chi^i_b, \text{and } x_{d \neq n} \in \chi\}. \quad (33)$$

As mentioned in [11], the complexity order of the simplified ML bit metrics (32) is proportional to M^D, i.e., $O(M^D)$. By using sphere decoding (SD), the average complexity reduces, but the worst-case scenario is still in the order of M^D, i.e., $O(M^D)$ [20]. Furthermore, for dimensions 2 and 4, the complexity can be reduced by separating the real part and imaginary part of $\tilde{\mathbf{y}}_{m,k}$. Note that in these cases, the matrix $\mathbf{R}$ is real. By doing this separation, the complexity order for the worst-case scenario reduces to $O(M^{\frac{D}{2}} - 0.5)$ [11].

V. Simulation Results

In the simulations, the industry standard 64-state 1/2-rate (133,171) $d_{\text{free}} = 10$ convolutional code is used. For BICMB, we separate the coded bits into different substreams of data and a random interleaver is used to interleave the bits in each substream. We assume that the number of RF chains in the receiver and transmitter are twice the number of data streams [7] (i.e., $N_t^{\text{RF}} = N_r^{\text{RF}} = 2N_s$). Also, each scale fading coefficient β_{ij} equals $\beta = -20$ dB for all simulations, except for Fig. 5. At RAUs in both the transmitter and the receiver, ULA array configuration with $d = 0.5$ is considered. Information bits are mapped onto 16-QAM symbols in each subchannel.

Fig. 2 illustrates the results for BICMB-PC for different values of D and L_{ij} in a mm-wave MIMO system. Furthermore, we can see the comparison of the BICMB-PC with

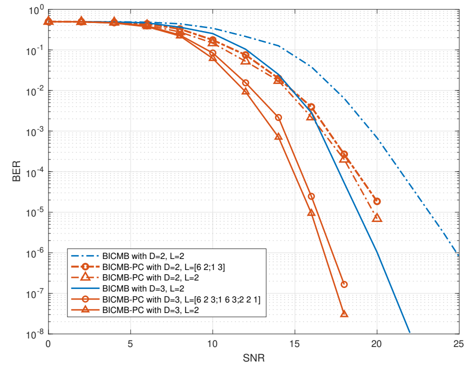

Fig. 2. BER with respect to SNR for setups. $N_t = 128$ and $N_r = 64$.

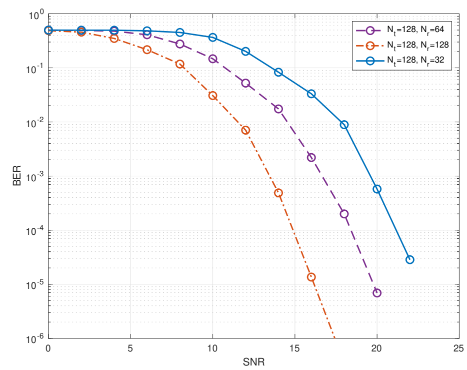

Fig. 3. BER with respect to SNR for different number of antennas at each RAU at the transmitter and receiver. $D = 2$ and $L = 2$.

the BICMB results in [7]. Please note that for the sake of comparison, $M_r = M_t = D$ in simulations related to [7], where M_r is the number of RAUs at the receiver side and M_t is the number of RAUs at the transmitter side. The number of propagation paths are defined as $\mathbf{L} = [L_{11}\ L_{12}; L_{21}\ L_{22}]$ and $\mathbf{L} = [L_{11}\ L_{12}\ L_{12}; L_{21}\ L_{22}\ L_{23}; L_{31}\ L_{32}\ L_{33}]$. When $\mathbf{L} = L$, all elements in $\mathbf{L}$ are constant and equal to L. It can be seen that the diversity gain remains the same for different values for the number of propagation paths, as long as (27) returns the same value of G_d. For example for the dashed-dot line curves with triangle markers and circle markers, since $\beta_{ij} = \beta$, the diversity gains can be calculated using (27). These calculated values are $G_d = 2 \times 2 \times 2$ and $G_d = (2 \times 2)^2/(6^{-1} + 2^{-1} + 3^{-1} + 1^{-1})$, respectively. It can be seen that the BICMB curves in [7] which are shown in Fig. 2 with blue curves with no markers, have the same slope in high SNR, i.e., same diversity gain as the BICMB-PC for different setups.

It can be seen from Fig. 3 that changing the number of antennas at the RAUs does not affect the diversity gain. This confirms (27) where the diversity gain is independent of the number of antennas at each RAU. Furthermore, one can see that by doubling the number of resources here, i.e., the number of antennas at the transmitter or the receiver, the performance of the system gets better by a factor of 3 dB.

In Fig. 4 we compare the results of this paper with a con-

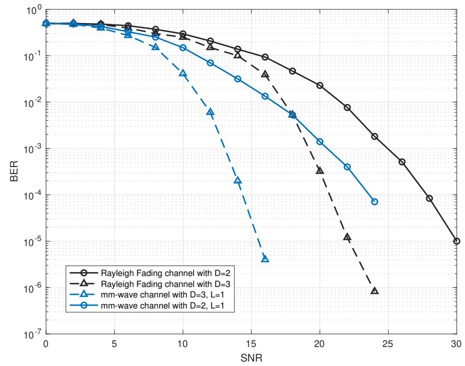

Fig. 4. BER with respect to SNR, comparing Rayleigh fading channel in [11] and Saleh-Valenzuela model for mm-wave channel in (5)

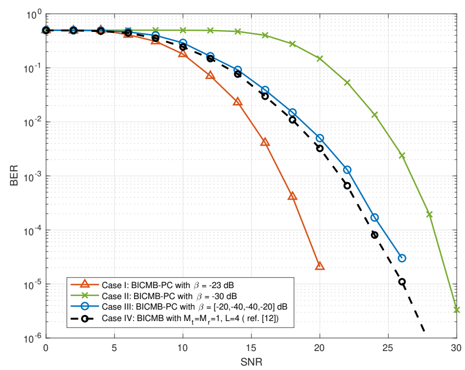

Fig. 5. BER with respect to SNR for different values of large scale fading coefficients. The black dashed curve is from [7] for the sake of comparison.

ventional MIMO system utilizing BICMB-PC with Rayleigh fading channel studied in [11]. In order to make these two comparable, we need to make the number of propagation paths in the channel to one, i.e., $L = 1$. Fig. 4 illustrates that for both cases when $D = 2$ and $D = 3$, the slope of the BER in high SNR for conventional MIMO system is the same as the the mm-wave model in (5).

Fig. 5 illustrates the effect of large scale fading coefficients on the diversity gain. We consider three different cases for BICMB-PC with $M_r = M_t = 2$, $L = 2$, and $N_s = 1$. Furthermore, in Case IV, we use BICMB in [7] where the diversity gain is $G_d \approx 4$ with $M_r = M_t = 1$, and $L = 4$. Let $\mathbf{B} = \left[\beta_{ij}\right]$ where β_{ij} expressed in dB, as the large scale fading coefficient matrix. We use the following matrices for the large scale fading coefficients for different cases:

$$\mathbf{B}_1 = \begin{bmatrix} -23 & -23 \\ -23 & -23 \end{bmatrix}, \mathbf{B}_2 = \begin{bmatrix} -30 & -30 \\ -30 & -30 \end{bmatrix},$$
$$\mathbf{B}_3 = \begin{bmatrix} -40 & -20 \\ -20 & -40 \end{bmatrix}, \mathbf{B}_4 = -20 \text{ dB}.$$

By using equation (27), one can see that the diversity gain for Case I and Case II is $G_d = 2\times2\times2 = 8$, whereas the diversity gain for Case III is $G_d = \frac{\left(10^{-4}+10^{-2}+10^{-2}+10^{-4}\right)^2}{10^{-8}/2+10^{-4}/2+10^{-4}/2+10^{-8}/2} \approx 4$. It can be seen from Fig. 5 that Case III has the same slope as Case IV, where both of them has a diversity gain of $G_d \approx 4$. One can see that in Case II, where the channel is inhomogeneous, the diversity gain decreases.

VI. Conclusion

In this work we showed that by utilizing BICMB-PC in a mm-wave MIMO system with DAS architecture, one can achieve full diversity gain. This means, the diversity gain is independent of the number of transmitted data streams and can be increased by increasing the number of RAUs at the transmitter or the receiver. We also show that the diversity gain is independent of the number of antennas at the RAUs in both the transmitter and the receiver. We leave the extension of the work to other STBC codes for future research.

References

[1] D. Yu, S. Xu, and H. H. Nguyen, "Diversity gain of millimeter-wave massive MIMO systems with distributed antenna arrays," *EURASIP Journal on Wireless Communications and Networking*, 2019.

[2] S. Ruan, B. Hu, K. J. Kim, Q. Li, L. Yuan, L. Jin, and J. Zhang, "Diversity analysis for spatial scattering modulation in millimeter-wave MIMO system," in *2019 11th International Conference on Wireless Communications and Signal Processing (WCSP)*, 2019, pp. 1–5.

[3] G. Caire, G. Taricco, and E. Biglieri, "Bit-interleaved coded modulation," *IEEE Trans. Inf. Theory*, vol. 44, no. 3, pp. 927–946, May1998.

[4] E. Zehavi, "8-PSK trellis codes for a Rayleigh channel," *IEEE Trans. Commun.*, vol. 40, no. 5, pp. 873–884, May 1992.

[5] E. Akay, E. Sengul, and E. Ayanoglu, "Bit interleaved coded multiple beamforming," *IEEE Trans. Commun.*, vol. 55, no. 9, pp. 1802–1811, Sep. 2007.

[6] H. J. Park and E. Ayanoglu, "Diversity analysis of bit-interleaved coded multiple beamforming," in *2009 IEEE International Conference on Communications*, June 2009, pp. 1–9.

[7] S. Sedighi and E. Ayanoglu, "Bit-interleaved coded multiple beamforming in millimeter-wave massive MIMO systems," *IEEE Trans. Commun.*, vol. 68, no. 10, pp. 6174–6185, 2020.

[8] F. Oggier, G. Rekaya, J. . Belfiore, and E. Viterbo, "Perfect space–time block codes," *IEEE Trans. Inf. Theory*, vol. 52, no. 9, pp. 3885–3902, Sep. 2006.

[9] G. Berhuy and F. Oggier, "On the existence of perfect space–time codes," *IEEE Trans. Inf. Theory*, vol. 55, no. 5, pp. 2078–2082, May 2009.

[10] B. Li and E. Ayanoglu, "Golden coded multiple beamforming," in *2010 IEEE Global Telecommunications Conference GLOBECOM 2010*, Dec 2010, pp. 1–5.

[11] ——, "Bit-interleaved coded multiple beamforming with perfect coding," in *2012 IEEE International Conference on Communications (ICC)*, June 2012, pp. 4246–4251.

[12] S. Li, J. Zhang, and X. Mu, "Double full diversity space time block code for massive MIMO system," in *2018 IEEE 10th Sensor Array and Multichannel Signal Processing Workshop (SAM)*, 2018, pp. 548–552.

[13] ——, "Noncoherent massive space-time block codes for uplink network communications," *IEEE Trans. Veh. Technol*, vol. 67, no. 6, pp. 5013–5027, 2018.

[14] J. G. Proakis and M. Salehi, *Digital Communications 5th Edition*. McGraw Hill, 2007.

[15] Z. Wang and G. B. Giannakis, "A simple and general parameterization quantifying performance in fading channels," *IEEE Trans. Commun.*, vol. 51, no. 8, pp. 1389–1398, Aug. 2003.

[16] H. Xu, V. Kukshya, and T. Rappaport, "Spatial and temporal characteristics of 60-GHz indoor channels," *IEEE J. Sel. Areas Commun*, vol. 20, no. 3, pp. 620–630, 2002.

[17] R. V. Hogg and A. T. Craig, *Introduction to Mathematical Statistics, 4th Edition*. New York: Macmillan, 1978.

[18] F. E. Satterthwaite, "An approximate distribution of estimates of variance components," *Biometrics B.*, vol. 2, no. 6, pp. 110–114, 1946.

[19] M. G. Bulmer, *Principles of Statistics*. Dover, 1965.

[20] J. Ahn, H. Lee, and K. Kim, "A near-ML decoding with improved complexity over wider ranges of snr and system dimension in MIMO systems," *IEEE Trans. Wireless Commun.*, vol. 11, no. 1, pp. 33–37, 2012.